Selective lowering of synapsins induced by oligomeric α-synuclein exacerbates memory deficits

Megan E. Larson[a,b,c,1], Susan J. Greimel[a,b,c,1], Fatou Amar[a,b,c], Michael LaCroix[a,b,c], Gabriel Boyle[a,b,c], Mathew A. Sherman[a,b,c], Hallie Schley[a,b,c], Camille Miel[a,b,c], Julie A. Schneider[d], Rakez Kayed[e], Fabio Benfenati[f,g], Michael K. Lee[a,c], David A. Bennett[d], and Sylvain E. Lesné[a,b,c,2]

[a]Department of Neuroscience, University of Minnesota, Minneapolis, MN 55414; [b]N. Bud Grossman Center for Memory Research and Care, University of Minnesota, Minneapolis, MN 55414; [c]Institute for Translational Neuroscience, University of Minnesota, Minneapolis, MN 55414; [d]Rush Alzheimer's Disease Center, Rush University Medical Center, Chicago, IL 60612; [e]Department of Neurology, University of Texas Medical Branch, Galveston, TX 77555; [f]Center for Synaptic Neuroscience, Istituto Italiano di Tecnologia, 16132 Genoa, Italy; and [g]Department of Experimental Medicine, University of Genova, 16132 Genoa, Italy

Edited by Solomon H. Snyder, The Johns Hopkins University School of Medicine, Baltimore, MD, and approved April 24, 2017 (received for review April 4, 2017)

Mounting evidence indicates that soluble oligomeric forms of amyloid proteins linked to neurodegenerative disorders, such as amyloid-β (Aβ), tau, or α-synuclein (αSyn) might be the major deleterious species for neuronal function in these diseases. Here, we found an abnormal accumulation of oligomeric αSyn species in AD brains by custom ELISA, size-exclusion chromatography, and nondenaturing/denaturing immunoblotting techniques. Importantly, the abundance of αSyn oligomers in human brain tissue correlated with cognitive impairment and reductions in synapsin expression. By overexpressing WT human αSyn in an AD mouse model, we artificially enhanced αSyn oligomerization. These bigenic mice displayed exacerbated Aβ-induced cognitive deficits and a selective decrease in synapsins. Following isolation of various soluble αSyn assemblies from transgenic mice, we found that in vitro delivery of exogenous oligomeric αSyn but not monomeric αSyn was causing a lowering in synapsin-I/II protein abundance. For a particular αSyn oligomer, these changes were either dependent or independent on endogenous αSyn expression. Finally, at a molecular level, the expression of synapsin genes *SYN1* and *SYN2* was down-regulated in vivo and in vitro by αSyn oligomers, which decreased two transcription factors, cAMP response element binding and Nurr1, controlling synapsin gene promoter activity. Overall, our results demonstrate that endogenous αSyn oligomers can impair memory by selectively lowering synapsin expression.

α-synuclein | oligomer | memory | Alzheimer's disease | synapsins

Although abnormal protein aggregates in the form of amyloid plaques, neurofibrillary tangles, and Lewy bodies (LB) characterize neurodegenerative disorders, such as Alzheimer's disease (AD) and Parkinson's disease, an accumulating body of evidence indicates that soluble multimeric species of these proteins, also known as oligomers, might underlie the deleterious cascades of molecular changes ultimately resulting in these chronic brain disorders (1–3). In this context, we define soluble endogenous amyloid oligomers as multimeric assemblies that (*i*) remain soluble in aqueous buffers following ultracentrifugation, (*ii*) are SDS-resistant following tissue lysis, (*iii*) are separated in liquid-phase chromatography, and (*iv*) are immunoreactive to at least two different antibodies for that amyloid molecule. Despite a well-accepted consensus that α-synuclein (αSyn) aggregation is critical for synaptic deficits, the exact relationship between various αSyn aggregation states and synaptic/cellular toxicity has not been formally established and remains a highly debated point of contention.

The normal function of αSyn remains poorly understood (4). It appears to be regulating the size of the presynaptic vesicle pool (5) and assisting in the formation of the SNARE complex (6, 7). Supporting this concept, overexpression of human WT αSyn (h-αSyn^{WT}) was shown to inhibit vesicle release, presumably through a reduction in the synaptic vesicle recycling pool, and a selective lowering of complexins and synapsins (8). Moreover, large multimeric assemblies of recombinant αSyn were recently shown to inhibit exocytosis by preferentially binding to synaptobrevin, thereby preventing normal SNARE-mediated vesicle docking (9). This point might be particularly important because αSyn was suggested to interact with synapsins, because of their colocalization and common association with the recycling pool, and as synapsin-I mediates the binding of recycling vesicles to the actin cytoskeleton (10, 11).

Beyond its physiological function, the native structure of αSyn has also been the subject of much debate (12–15). Briefly, the native state of αSyn was believed for a long time to be an unfolded ∼14-kDa monomer that only acquired an α-helical structure upon binding to lipids (16). However, several recent studies challenged this notion, claiming that the native state was primarily a folded tetramer of ∼58 kDa (15, 17). Given that the native tetramer was not prone to aggregation, these authors concluded that the oligomeric and fibrillar forms likely result from destabilization of the apparent αSyn tetramer (15). Other studies have, however, challenged the existence of a native tetrameric αSyn, concluding that endogenous αSyn purified from brain tissue consists of a largely unstructured monomer and is prone to aggregation (12, 14). Altogether, the consensus appears to be that αSyn may exist as monomers and soluble physiological multimers

Significance

Alzheimer's disease (AD) is the most common form of dementia affecting an estimated 5.3 million Americans based on the 2015 Report of the Alzheimer Association. Our current understanding of the pathogenesis of AD suggests that soluble, nonfibrillar forms of amyloid proteins [e.g. amyloid-β, tau, and α-synuclein (αSyn)] may be responsible for impairing cognition and have therefore been advanced to be the most bioactive species in this brain disorder. We sought to determine the potential contribution of αSyn oligomers to AD-associated cognitive decline. We found that selective αSyn oligomers are elevated in AD brains and that genetically elevating oligomeric αSyn in an AD mouse model led to a selective decrease in presynaptic proteins and cognitive performance.

Author contributions: M.K.L., D.A.B., and S.E.L. designed research; M.E.L., S.J.G., F.A., M.L., G.B., M.A.S., H.S., C.M., and S.E.L. performed research; J.A.S., R.K., F.B., M.K.L., D.A.B., and S.E.L. contributed new reagents/analytic tools; M.E.L., S.J.G., F.A., M.L., G.B., M.A.S., H.S., C.M., J.A.S., R.K., F.B., D.A.B., and S.E.L. analyzed data; and M.E.L. and S.E.L. wrote the paper.

The authors declare no conflict of interest.

This article is a PNAS Direct Submission.

[1]M.E.L. and S.J.G. contributed equally to this work.

[2]To whom correspondence should be addressed. Email: lesne002@umn.edu.

This article contains supporting information online at www.pnas.org/lookup/suppl/doi:10.1073/pnas.1704698114/-/DCSupplemental.

www.pnas.org/cgi/doi/10.1073/pnas.1704698114

in cells, and that some forms of αSyn oligomers (*o*-αSyn) may be responsible for toxicity (4).

We previously reported that the abundance of soluble, intracellular (IC) αSyn monomers was increased in AD brain tissue compared with controls in the absence of apparent LBs. Moreover, the amounts of IC monomeric αSyn in temporal cortices translated into a better biological correlate of AD-associated cognitive impairment than soluble amyloid-β (Aβ) and tau (18). Finally, the threefold overexpression of h-αSyn^{WT} was sufficient to trigger memory deficits in 7-mo-old transgenic (Tg)I2.2 mice in the absence of αSyn cytopathology (18). At a cellular level, the elevation of IC monomeric αSyn observed in AD coincided with selective reductions in two presynaptic proteins, synapsin and complexin, and with a perturbed colocalization of αSyn and synapsins within presynaptic vesicles (18), in agreement with previous reports (8, 19, 20). These observations therefore suggested a possible connection between the dysregulation of αSyn expression and alterations in presynaptic vesicle composition and release.

It is in this uncertain context that we sought to determine whether an aberrant formation of *o*-αSyn accompanying the changes in monomeric αSyn previously seen in our AD cohort (18) was contributing to the decrease in synapsins and enhanced memory deficits. In the present study, we found that selective *o*-αSyn species accumulated in AD brain tissue in the absence of IC LB pathology. In particular, we observed that ∼28- to 35- and ∼56-kDa αSyn species (putative dimers and tetramers, respectively) were elevated by ∼1.5- to 2-fold, consistent with the 1.7- to 2.3-fold elevation previously documented for monomeric αSyn (18). Using biochemical and immunological approaches, we confirmed the oligomeric nature of these αSyn assemblies and observed that the abundance of *o*-αSyn species was inversely correlated with synapsins and cognitive function in our human cohort. To test whether elevating endogenous soluble h-αSyn^{WT} oligomers was sufficient to induce enhanced cognitive deficits and a selective reduction in synapsins in a mouse model of AD (21), we created a bigenic mouse line overexpressing mutant human amyloid precursor protein (APP) and h-αSyn^{WT}, with the intent that Aβ would promote the aggregation of αSyn (22). In this new APP/αSyn line, the oligomerization of αSyn was increased by fourfold, accompanied by a selective decrease of synapsins and by an exacerbation of Aβ-induced cognitive deficits. Finally, IC delivery of isolated endogenous *o*-αSyn, but not monomeric αSyn, in primary cortical neurons specifically triggered a decrease in synapsin expression. Overall, our data indicate that oligomeric αSyn-mediated lowering in synapsins might enhance AD-associated cognitive deficits.

Results

Elevation of Soluble αSyn Oligomers in AD Brain. To determine whether *o*-αSyn might be elevated in parallel to the increase in IC monomeric αSyn previously reported (18), in the absence of LB pathology (Fig. S1), we created an in-house ELISA to detect soluble multimers of αSyn by homotypic recognition and soluble αSyn conformers immunoreactive to the A11 antibody (Fig. 1*A*). Using both detection sets, oligomeric αSyn species were elevated in AD subjects compared with age-matched, noncognitively impaired controls (NCI) by 34% and 48%, respectively (Fig. 1 *B*–*D*). Similar changes were detected in the mild cognitive impairment (MCI) group, albeit overall lower (Fig. 1 *C* and *D*). The selectivity and sensitivity of the assay was confirmed by comparing increasing concentrations of recombinant monomeric or oligomeric αSyn (rec-hαSyn^{WT}) and using brain lysates from WT, TgI2.2, and *SNCA*-null mice (Fig. S1). For a large proportion, the abundance of soluble αSyn assemblies was detected similarly well by the homotypic LB509-LB509 and heterotypic LB509-A11 sets, as indicated by the correlation observed between brain levels of LB509^{+} *o*-αSyn and A11^{+} *o*-αSyn species (Spearman's $\rho = 0.487$, $P < 0.0001$, $n = 84$) (Fig. 1*E*).

To determine the size of the putative soluble *o*-αSyn detected, we combined size-exclusion chromatography (SEC) with antibody detection under denaturing or native conditions. Western blotting analyses of isolated SEC fractions using IC-enriched

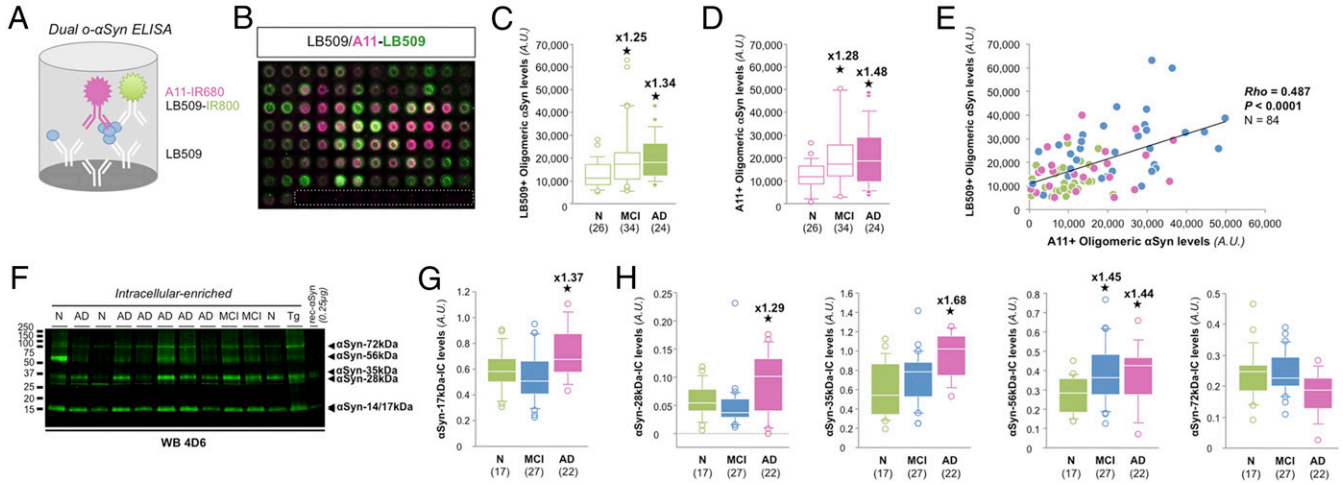

Fig. 1. Identification of soluble αSyn assemblies in human brain tissues. (*A*) Experimental design of oligomeric αSyn ELISA. The capture antibody consisted in the human specific αSyn antibody LB509 and a tandem of detecting antibodies (LB509-IR800 and A11-Biotin) was used to reveal oligomeric αSyn. (*B*) Representative infrared images of oligomeric αSyn measurements in Religious Orders Study specimens ($n = 84$) using either LB509-LB509 (homotypic) or LB509-A11 sandwiches on 96-well ELISA plates. Each well represents a separate patient sample. The dashed rectangle indicates increasing amounts of freshly resuspended recombinant monomeric αSyn (last row, samples 86–96, 1 pg to 10 ng). Please note that no signal was detected confirming the specificity of the assay. (*C* and *D*) Box plots for oligomeric αSyn species using either the homotypic LB509 sandwich (*C*) or the LB509-A11 sandwich (*D*). Obvious differences were observed between the AD group ($n = 24$) and the NCI (N) group ($n = 26$). (Mann–Whitney *U* test, $F_{1,\ 47} = 4.9728$ and $F_{1,\ 47} = 5.0115$, respectively; Student *t* test, $^{\star}P < 0.05$ vs. NCI.) (*E*) Regression analyses indicated a positive correlation between oligomeric αSyn species detected with either LB509/LB509 (*x* axis) or with LB509/A11 (*y* axis) ($n = 84$; Spearman rank correlation, $P < 0.0001$). (*F*) Western blot (WB) analyses of soluble αSyn species in IC-enriched fractions using 4D6. Tg mice from the TgI2.2 line and recombinant human αSyn^{WT} were used as positive controls. (*G* and *H*) Box plots for monomeric (*G*) and putative oligomeric (*H*) αSyn species in the temporal cortex of subjects with NCI, MCI, or AD devoid of αSyn inclusions. Numbers in parentheses indicate group sizes. NCI is shown in green, MCI in blue, and AD in magenta boxes. In box plots of all figures, the bar inside the box indicates the median; the upper and lower limits of boxes represent the 75th and 25th percentiles, respectively. Bars flanking the box represent the 95th and fifth percentiles. (Kruskal–Wallis followed by Mann–Whitney *U* test, $F_{1,\ 66} = 4.2289$, $F_{1,\ 66} = 4.4464$, $F_{1,\ 66} = 4.7717$, $F_{1,\ 66} = 3.8853$, and $F_{1,\ 66} = 2.4774$ respectively; $^{\star}P < 0.05$ vs. NCI.) A.U., arbitrary units.

lysates from AD individuals with normal (AD-normal) or high (AD-high) levels of αSyn (18) revealed the presence of various soluble αSyn species (Fig. S2). In contrast, freshly resuspended monomeric rec-hαSyn^{WT} did not behave as a globular protein in the SEC column because of its disordered structure, resulting in its elution at fractions 49–53 instead of fractions 61–63 (Fig. S3*A*), in line with earlier observations (12, 14, 15). AD brain-derived αSyn monomers eluted in fractions 43–53, likely because of the presence of two distinct 17- and 14-kDa monomeric forms (Fig. S2*A*). This finding was also observed in TgI2.2 mice overexpressing h-αSyn^{WT} (Fig. S3*B*). In addition, we noticed the presence of putative SDS-resistant αSyn species in Tg mouse and human brain lysates that appeared to behave as globular proteins (Figs. S2*A* and S3*B*). Several 4D6-immunoreactive bands of ∼28, 35, 56, and 72 kDa were readily detected, consistent with potential dimers and tetramers of the 14- and 17-kDa αSyn monomers mentioned above. Of note, the putative 28-kDa dimer eluted at its predicted globular molecular weight and did not coelute with any other detectable αSyn species (considering a detection limit for αSyn of ∼2.5 pg). This observation also argued against the possibility that this assembly was the result of a breakdown of a larger structure or of a self-aggregation of αSyn monomers. Quantitative densitometry analysis revealed significantly higher amounts of the 17- and 28-kDa species (a 1.42- and 2.23-fold elevation, respectively) in AD-high subjects compared with AD-normal (Fig. S2*B*), suggesting a differential elevation of *o*-αSyn in AD and intrinsically validating the results reported earlier by our group (18).

To further characterize the oligomeric nature of these soluble αSyn species, we performed nondenaturing analyses of SEC fractions by dot-blotting assay using IC-enriched extracts from AD-high, TgI2.2, WT, and *SNCA*-null mice (Fig. S4). Each fraction was subjected to a panel of commercially available antibodies detecting human αSyn (LB509, 4B12), mouse/human αSyn (4D6), phosphorylated and misfolded αSyn (pS129-αSyn and Syn514), and to a panel of antibodies generated to detect oligomeric and aggregated amyloid proteins (A11, OC, Officer), including *o*-αSyn (Syn33, F8H7) (23). We also included analyses with the 6E10 antibody detecting $A\beta_{1-16}$ to determine whether the putative *o*-αSyn might be coupled to Aβ as a hybrid oligomer (24). Although a clear signal was detected in fraction 38, likely because of soluble APP or Aβ protofibrils, the pattern obtained with 6E10 was distinct from those found with αSyn antibodies. LB509 and 4B12 antibodies readily detected isolated monomeric αSyn in AD and TgI2.2 fractions, but not in either WT or *SNCA*-null fractions (Fig. S4*A*, lane 2). However, under these experimental settings, both proved quite poor at detecting αSyn in SEC fractions containing apparent *o*-αSyn (Fig. S4*A*, lanes 3–4). Using 4D6 modestly improved detection (Fig. S4*A*, lanes 3–4). We hypothesized that the 4D6 epitope was partly available because of the conformation of the putative *o*-αSyn species. To relax the folding of the protein, we boiled nitrocellulose membranes onto which samples had been previously preadsorbed. Under these new conditions, the detection of αSyn with 4D6 was substantially improved, revealing the presence of αSyn assemblies, consistent with 28-kDa dimers and cosegregated 35-kDa/72-kDa multimers (Fig. S4*A*). To confirm that these species corresponded to αSyn oligomers, we used antibodies detecting various oligomers of amyloid proteins (i.e., A11, OC, Officer) (25, 26), as well as antibodies specific to *o*-αSyn, Syn33, and F8H7 (23). OC and Officer detected fibrillar amyloid species cosegregating with the 35-kDa/72-kDa αSyn molecules in both AD and TgI2.2 samples, suggesting that the αSyn forms detected in SEC fraction 38 were prefibrillar oligomeric αSyn assemblies. In contrast, the 28-kDa αSyn dimers were detected with A11 and F8H7 in AD brain tissue and to a lesser extent in TgI2.2 mice, indicating that this αSyn species is indeed a nonfibrillar oligomer. Of note, we observed a faint immunoreactivity of SEC fraction 38 in the WT samples by antibodies 4D6 (boiled) and F8H7 (Fig. S4*A*), likely indicating the existence of physiological multimeric αSyn assemblies. As expected, the same analysis performed with *SNCA*-null mouse tissue did not yield any signal. In addition, SEC fractions containing the apparent 72-, 17-, and 28-kDa αSyn species isolated from either AD-normal or AD-high groups were subjected to the *o*-αSyn ELISA and confirmed the selective increase in discrete *o*-αSyn species (i.e., 28-kDa αSyn) (Fig. S4*B*).

To demonstrate that these 4D6-immunoreactive molecules corresponded to *o*-αSyn, we turned to TgI2.2 mice, a simpler model in which h-αSyn^{WT} is overexpressed. As previously reported, these animals did not display LB pathology (Fig. S5*A*). An age-dependent increase of the same αSyn species detected in AD brain tissue was observed in brain lysates of TgI2.2 mice at 4, 7, and 11 mo of age compared with WT and knockout littermates (Fig. S5 *B* and *C*). Of note, monomeric αSyn also increased with aging (Fig. S5*D*). We then subjected TgI2.2 IC fractions to hexafluoroisopropanol (HFIP) to promote the disassembly of putative *o*-αSyn into soluble αSyn monomers (Fig. S5 *E* and *F*). Low concentrations of HFIP (10–20%) appeared to trigger the oligomerization of low-molecular weight (LMW) αSyn species, as evidenced by the detection of larger species immunoreactive to 4D6 creating the appearance of a smear in the upper parts of the SDS/PAGE gel and by the reduction in the abundance of putative low-*n* *o*-αSyn. Increasing HFIP concentration to 100% induced the destruction of the quaternary structure of *o*-αSyn multimers into monomeric αSyn molecules (Fig. S5 *E* and *F*). It is worth noting that the 72-kDa band remained partially unaffected by this treatment, consistent with the detection of a faint band in IC protein lysates from *SNCA*-null mice (Figs. S3 and S5). Overall, these results indicate that the αSyn assemblies detected by 4D6 are indeed oligomeric in nature.

With the identification of 4D6 as the most sensitive antibody to detect *o*-αSyn under denaturing conditions (Figs. S4 and S5), we then reanalyzed the extracellular (EC)- and IC-enriched fractions of human brain specimens previously characterized using LB509 (18). As hypothesized, apparent SDS-resistant *o*-αSyn were readily detected by 4D6 in IC and EC fractions (Fig. 1 *F* and *G* and Fig. S6, respectively). In agreement with earlier results from our own group, we did not find differences in soluble EC αSyn monomers between clinical groups (Fig. S6 *A* and *B*). In contrast, soluble αSyn species of ∼17, 28, and 56 kDa were, respectively, elevated by 1.64-, 1.75-, and 1.64-fold in the IC fraction of AD subjects compared with NCI individuals (Fig. 1 *G* and *H*) and reduced in the EC fractions of these brain tissues (Fig. S6 *A* and *B*). Interestingly, a rise of the ∼56-kDa αSyn species was also detected in brain tissue from individuals diagnosed with MCI compared with NCI. Finally, these changes did not appear to be limited to the inferior temporal gyrus as other brain regions (angular gyrus, entorhinal cortex) also displayed elevations in apparent *o*-αSyn (Fig. S6 *C*–*G*). Clearly, larger studies will be needed in the future to extensively compare regional differences within each subject.

Altogether, our data suggest that specific LMW *o*-αSyn species can accumulate in AD in absence of LB pathology.

O-αSyn Species Negatively Correlate with Measures of Cognitive Performance. To determine whether the elevation in soluble *o*-αSyn species identified in AD brain tissue might be associated with cognitive deficits, we performed multivariable regression analyses using all measurements of soluble forms of αSyn detected with either 4D6 or LB509 and measures of cognitive function (Fig. 2). Analyzed cognitive domains included episodic, semantic, and working memory, visuospatial ability, perceptual speed, and global cognition. Following multivariate regression analyses, color maps for correlation indexes revealed that neither EC nor IC *o*-αSyn were correlated with cognition in age-matched controls (Fig. 2*A*, *Left color maps*). In contrast, we observed that inferior temporal gyrus (ITG) levels of putative 28-, 35-, and 56-kDa *o*-αSyn were inversely correlated with episodic memory deficits ($\rho = -0.661$, $P = 0.0376$; $\rho = -0.833$, $P = 0.0098$, and $\rho = -0.556$, $P = 0.0203$, respectively) (Fig. 2*A*, *Right color map*). Overall, there was a generalized trend toward an inverse correlation between cognitive function and all IC αSyn species in our AD

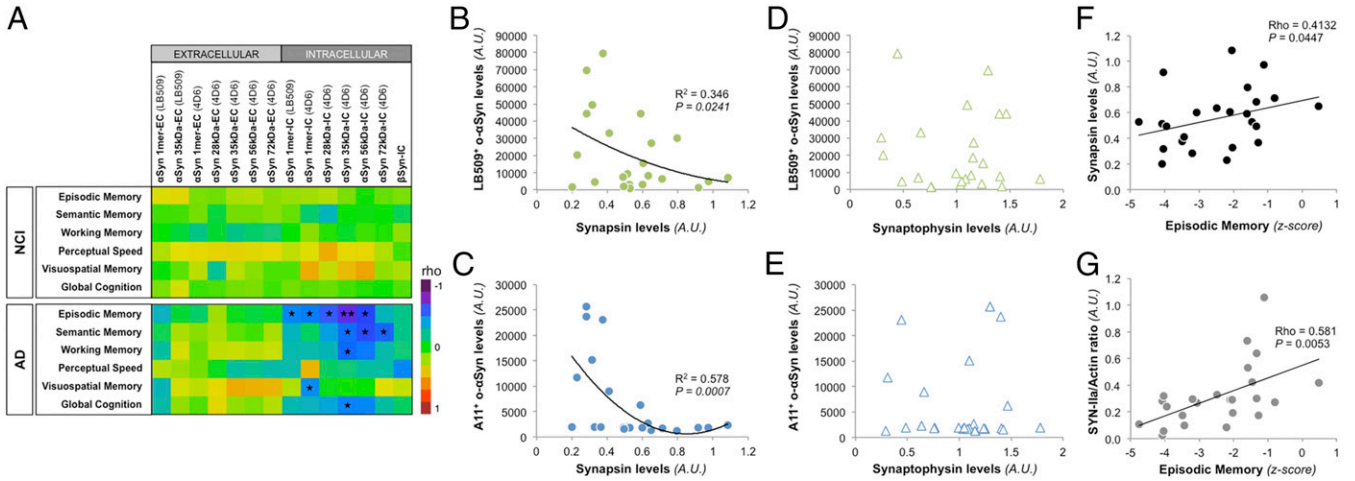

Fig. 2. Soluble αSyn assemblies are associated with changes in cognitive function and synaptic expression in AD. (*A*) Following the measurements of soluble αSyn species in EC- and IC-enriched fractions of human temporal cortices, multivariate analysis was performed within the NCI and AD groups. Monomeric αSyn expression was used as positive control (18) and βSyn expression was used as negative control. Finally, all measures of proteins were performed using the same technique (SDS/PAGE followed by Western blot) to avoid inherent differences between techniques. Raw measurements of all proteins were used for the analysis. (Spearman's ρ correlation with Bonferroni correction, $^{\star}P < 0.05$; $^{\star\star}P < 0.01$, $n_{NCI} = 26$ and $n_{AD} = 24$). (*B* and *C*) Regression analyses between total synapsin protein expression and *o*-αSyn measured by ELISA using either LB509 (*B*) or A11 (*C*) as the detecting antibody in all AD cases tested ($n = 24$). Best-fitting models indicated significant negative correlations for both *o*-αSyn measurements (Spearman's ρ, $\rho = -0.346$, $P = 0.0241$ and $\rho = -0.551$, $P = 0.0052$ respectively, $n = 24$). (*D* and *E*) Regression analyses between SYP protein expression and *o*-αSyn measured by ELISA using either LB509 (*D*) or A11 (*E*) as the detecting antibody revealed no correlations between *o*-αSyn and SYP (Spearman's ρ, $\rho = -0.1745$, $P = 0.4248$ and $\rho = -0.1470$, $P = 0.4932$ respectively, $n = 24$). (*F* and *G*) Regression analyses revealed positive correlations between synapsin levels, total (*F*) or isoform specific (*G*), and episodic memory performance in our AD cohort (Spearman's ρ, $\rho = 0.4132$, $P = 0.0447$ and $\rho = 0.581$, $P = 0.0053$ respectively, $n = 24$). A.U., arbitrary units.

group. In agreement with our earlier studies (18), we found that levels of IC monomeric αSyn were inversely correlated to episodic memory and visuospatial ability, despite using a different antibody to measure αSyn (i.e., 4D6 instead of LB509).

Brain Levels of Soluble αSyn Oligomers Correlate with a Selective Lowering in Synapsins I/II. The overexpression of h-αSyn^{WT} is associated with a selective reduction in synapsins and complexins in mice (8). Given that large *o*-αSyn species were recently proposed to inhibit the docking of synaptic vesicles (9) and that synapsins regulate synaptic transmission and plasticity, we hypothesized that the increase in *o*-αSyn measured in our AD cohort could be related to the decrease in synapsins reported earlier (18). Measuring synapsin protein expression by Western blotting (8, 18), we found that the abundance of *o*-αSyn measured by ELISA using LB509 as the detection antibody inversely correlated with total levels of synapsin isoforms (Ia/b and IIa/b) in the ITG ($R^2 = -0.346$, $P = 0.0241$) (Fig. 2*B*). Similarly, A11$^+$ *o*-αSyn amounts correlated with the lowering in synapsin expression in AD brains ($R^2 = -0.578$, $P = 0.0007$) (Fig. 2*C*), although to a greater extent than LB509$^+$ αSyn quantitatively. To assess whether these relationships were specific to synapsins, we performed additional regression analyses using the protein abundance of other presynaptic markers, such as synaptophysin (SYP). Consistent with previous reports, SYP protein levels were reduced in AD compared with age-matched controls (Fig. S7 *A* and *B*) and correlated with global cognition (Fig. S7*C*). However, no correlations were found between *o*-αSyn and SYP using either ELISA detection pairs (Fig. 2 *D* and *E*). These data suggest that the elevation of *o*-αSyn in AD might alter synapsin expression or turnover.

Oligomeric αSyn-Associated Lowering of Synapsin-I/II Correlates with Memory Impairment. We then determined whether the observed reduction in synapsins might be associated with episodic memory deficits, because this memory modality is specifically affected in AD (Fig. 2 *F* and *G*). We found that greater deficits in episodic memory correlated with lower total synapsin (-I/II) levels (Spearman's $\rho = 0.4132$; $P = 0.0447$). Comparisons between synapsin isoforms (Ia, Ib, IIa, and IIb) further validated this trend as shown for SYN-IIa and episodic memory (Spearman's $\rho = 0.581$; $P = 0.0053$) or other memory modalities (Fig. S7 *D* and *E*).

We previously reported that 7-mo-old TgI2.2 mice present with spatial reference memory deficits (18). As shown in Fig. 3 and Figs. S3 and S5, despite the faint detection of *o*-αSyn in the forebrain of 3- to 4-mo-old TgI2.2 animals, the protein abundance of synapsin isoforms was similar to that of WT mice (Fig. S8 *A* and *B*). Other presynaptic proteins, such as complexins, Rab3, and SYP were also indistinguishable between genotypes at that age. However, at ages when TgI2.2 mice are cognitively impaired in the Barnes circular maze (BCM) (18), we observed a 30–40% reduction of synapsin proteins at 7 mo, compared with WT mice, and an exacerbation of these changes at 11 mo of age (Fig. S8 *C* and *D*). Furthermore, transcriptional analysis of *SYN1*, *SYN2*, *CPLX1*, *CPLX2*, *SYP*, and *SYT* mRNAs revealed a selective down-regulation of synapsin transcripts with aging in TgI2.2 mice (Fig. S8*E*). These findings suggest an association between αSyn, synapsin expression, and memory function.

Enhancing αSyn Oligomerization in an AD Mouse Model Alters Synapsin Expression and Synaptic Localization. Because both monomeric and oligomeric αSyn increase with age in TgI2.2 mice (Fig. S4), thereby preventing the identification of putative changes linked to one or the other, we created a bigenic mouse line by crossing J20 mice (21) with TgI2.2 mice (27) to test whether an elevation in soluble h-αSyn^{WT} oligomers was sufficient to induce a selective reduction of synapsins in a mouse model of AD. Because Aβ and αSyn are known to promote the aggregation of each other in vivo (22, 28), we expected to trigger the oligomerization of αSyn when Aβ is overexpressed. We observed that the expression of transgene-derived h-αSyn^{WT} monomers was similar between TgI2.2 and J20×TgI2.2 mice (Fig. 3 *A* and *B*). However, we noticed a 3.7-fold increase in LMW *o*-αSyn in bigenic mice compared with TgI2.2 at 3 mo of age (Fig. 3 *A* and *B*). Importantly, we did not observe expression changes in APP and Aβ in these animals (Fig. S9 *A* and *B*) nor formation of amyloid deposits (Fig. S9*C*). This specific profile

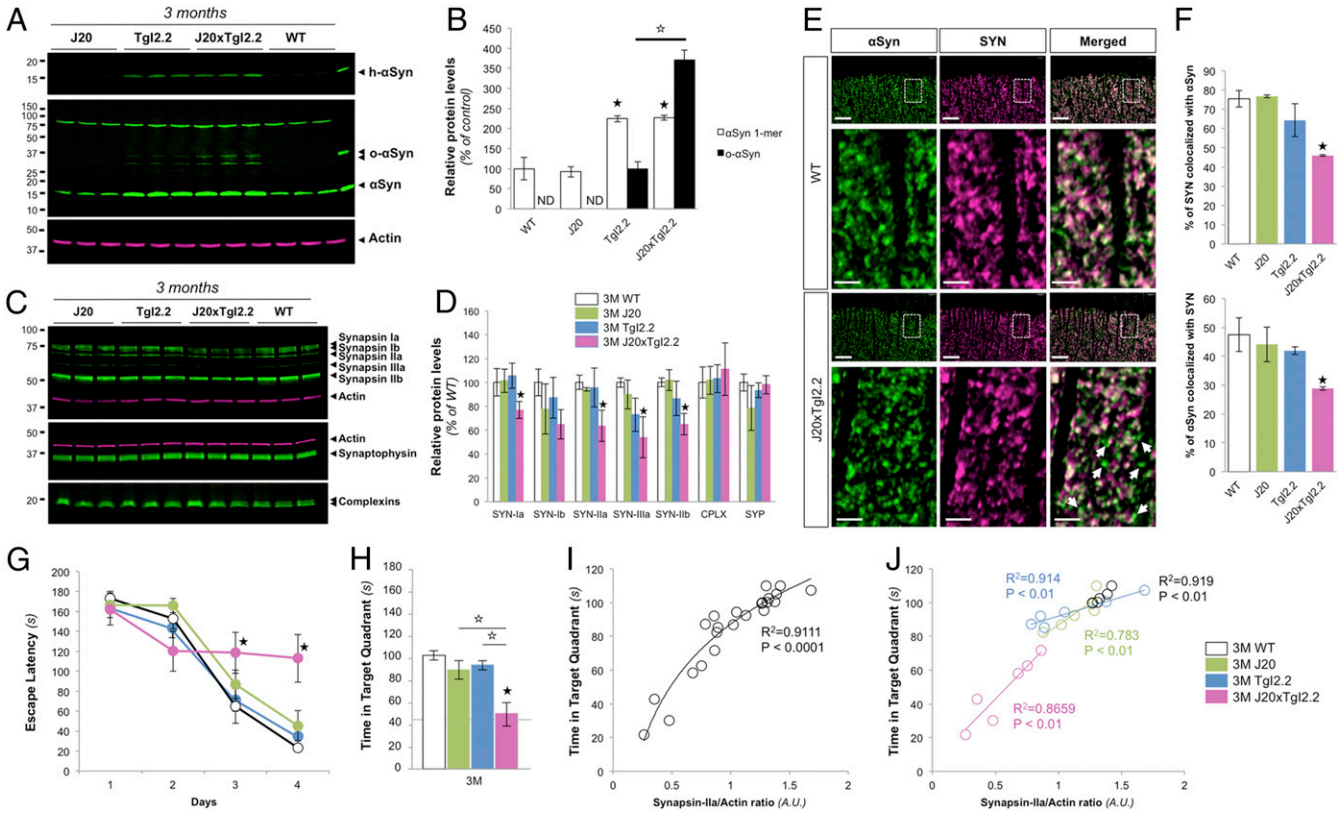

Fig. 3. Genetic elevation of oligomeric αSyn in the J20 mouse model of Alzheimer's disease is associated with a selective reduction in synapsin expression and exacerbated cognitive deficits. Three-month-old non-Tg WT, J20, Tgl2.2, and J20×Tgl2.2 mice were analyzed in the BCM. Immediately following behavioral testing, mice were killed for gene and protein analyses. (*A*) Representative Western blot images for transgene-derived human αSyn and total αSyn (mouse and human) using forebrain IC lysates. Actin was used as internal control. (*B*) Quantification of αSyn species revealed a significant elevation of putative *o*-αSyn in J20×Tgl2.2 mice at 3 mo (ANOVA followed by Student *t* test with Bonferroni correction, $F_{3,\ 24} = 754.193$, $^{\star}P < 0.05$ vs. WT, $^{\star}P < 0.05$ vs. Tgl2.2, $n = 6$ per age per genotype). (*C*) Representative Western blot images for synapsins and SYP using forebrain MB lysates. Actin was used as internal control. (*D*) Densitometry analyses confirmed the apparent visual reduction in synapsins in bigenic J20×Tgl2.2 mice compared with other mouse groups (ANOVA followed by Student *t* test with Bonferroni correction, $^{\star}P < 0.05$ vs. WT, $n = 6$ per age per genotype). (*E*) Double labeling for αSyn (green) and synapsins (magenta) in 6-μm-thick sections of the CA1 domain of the hippocampus from 3-mo-old WT and J20×Tgl2.2 mice. (Scale bars: 20 μm, *Upper*; 4 μm, *Lower*.) (*F*) Quantification of the colocalization between αSyn/SYN in the stratum radiatum of WT, J20, Tgl2.2, and J20×Tgl2.2 mice using Bitplane's Imaris7.x colocalization tool. *Z*-stacks of images were transformed for volume rendering and voxel count analysis was performed. (Histogram values represent mean ± SD, ANOVA followed by Student *t* test with Bonferroni correction, $F_{3,\ 48} = 167.576$ and, $F_{3,\ 48} = 64.229$, $^{\star}P < 0.05$ vs. WT, $n = 6$ animals, 8 fields per mouse.) (*G*) Three-month-old non-Tg C57BL/6, J20, Tgl2.2, and J20×Tgl2.2 mice were trained in the BCM for 4 d. A probe trial (escape platform removed) was conducted 24 h after the last training session. During acquisition of the task, escape latency to complete the task was recorded. Although J20 and Tgl2.2 groups learned this task comparably to WT mice, J20×Tgl2.2 bigenic mice displayed a severe acquisition deficit. In these mice, two-way repeated-measures ANOVA (RMANOVA) revealed an effect of transgene ($F = 36.89$, $P = 0.0008$) but no significant effect of training ($F = 8.02$, $P = 0.8236$). Although different from WT animals, J20×Tgl2.2 mice were partly able to learn the task ($^{\star}P < 0.05$ vs. WT mice). (*H*) During the probe trial, J20×Tgl2.2 animals did not elicit a spatial search bias compared with WT and single Tg littermates. Bigenic J20×Tgl2.2 mice consistently performed worse than age-matched single Tg J20 and Tgl2.2 animals (two-way ANOVA, $^{\star}P < 0.05$ vs. WT mice; $^{\star}P < 0.05$ vs. J20×Tgl2.2 mice). Data represent mean ± SEM ($n = 6$–8 males per age per genotype). (*I*) Relationship between probe trial performance and relative synapsin-IIa expression in all animals tested. The best fit is represented on the dot plot ($R^2 = 0.9111$, $P < 0.0001$, $n = 24$). (*J*) Regression analyses between probe trial performance and relative synapsin-IIa expression by genotype of tested animals revealed linear relationships within each group, including bigenic J20×Tgl2.2 mice ($R^2 = 0.8659$, $P < 0.01$, $n = 6$ animals). A.U., arbitrary units.

allowed us to test whether the ∼fourfold elevation in *o*-αSyn was associated with a selective decrease in synapsins. Although no overt changes in SYP and complexins were observed across all mouse genotypes, a reduction in synapsins was readily visible in J20×Tgl2.2 bigenic mice compared with J20, Tgl2.2, and WT animals (Fig. 3*C*). Densitometry analysis revealed significant decreases of synapsin Ia, IIa, IIIa, and IIb in the forebrain of bigenic mice with no apparent changes in SYP or complexins (Fig. 3*D*).

We and others have previously reported that when αSyn is accumulating, its colocalization with synapsins at synaptic boutons is altered (8, 18, 20). However, the potential contribution of *o*-αSyn to this phenomenon is unknown. We therefore examined the colocalization of synapsins with αSyn in the stratum radiatum of the CA1 region of the hippocampus in 3-mo-old WT, J20, Tgl2.2, and J20×Tgl2.2 mice (Fig. 3 *E* and *F*). Confocal image analysis revealed a ∼40% reduction in the colocalization of αSyn with synapsins in bigenic animals compared with controls (Fig. 3*F*).

Overall, these findings suggest that *o*-αSyn might selectively regulate the expression, cellular targeting, and turnover of synapsin proteins.

Elevating *o*-αSyn Exacerbates Memory Deficits in APP Mice. To determine whether the increase in *o*-αSyn and its associated decrease in synapsins exacerbated Aβ-induced cognitive deficits, we subjected all four animal groups to behavioral testing using the BCM to assess spatial reference memory at 3 mo of age (Fig. 3*G*). Bigenic J20×Tgl2.2 animals displayed an apparent delay in learning the task compared with WT and single Tg J20 and

TgI2.2 littermates (Fig. 3*G*). During the retention trial on day 5, J20×TgI2.2 mice did not show a search bias to the target hole whereas all other age-matched groups performed similarly (Fig. 3*H*). Regression analyses revealed positive correlations between synapsin isoform expression and memory integrity, as exemplified by results obtained for synapsin IIa across all animals (Fig. 3*I*) or within genotype (Fig. 3*J*). These results suggest that learning and spatial memory recall were affected in plaque-free J20×TgI2.2 mice in presence of elevated *o*-αSyn.

IC Delivery of Exogenous *o*-αSyn Lowers Synapsin Protein Abundance. To demonstrate that *o*-αSyn were responsible for altering synapsin protein abundance, we sought for means to deliver *o*-αSyn isolated from brain tissues inside primary cortical neurons. Using the shuttling reagent Chariot (Active Motif), we first successfully established the principle that we could deliver large molecules: for example, fluorescently labeled antibodies, intracellularly (Fig. S10*A*). We then prepared preparations of rec-hαSyn^{WT}, which were segregated by SEC to obtain preparations enriched in αSyn monomers or oligomers (Fig. S10*B*). Six hours postdelivery, primary neurons that received rec-hαSyn^{WT} monomers displayed enhanced expression of monomeric αSyn, whereas cells that received rec-hαSyn^{WT} oligomers readily contained *o*-αSyn without noticeable changes in cell-derived αSyn monomers (Fig. S10*C*). Under these experimental conditions, no apparent changes in synapsin abundance were observed upon IC delivery of rec-hαSyn^{WT} (Fig. S10 *D* and *E*). Because the folding of αSyn might differ in vitro compared with that occurring in vivo, we isolated soluble αSyn species from 11-mo-old TgI2.2 mice by SEC (Fig. 4*A*). We selected to test whether fractions enriched in αSyn monomers (#48), low-*n* oligomers (#56), or larger oligomers (#38) could lower synapsin protein abundance in vitro. To confirm the absence of multimeric assembly in SEC fraction #48, we performed independent nondenaturing analyses of SEC fraction #48 by Clear Native-PAGE, in which we did not observe the presence of multimeric species (Fig. S10*F*). Vehicle, fractions that do not contain αSyn (#36) or corresponding fractions from *SNCA*-null mice were used as negative control. Immunofluorescence labeling of exogenous αSyn species confirmed the IC delivery of h-αSyn into cultured primary neurons (Fig. 4*B*). Accordingly, we found that the protein amounts of synapsin-I and -II were not changed in cells that received intraneuronal delivery of αSyn monomers (#48) compared with vehicle-treated neurons (Fig. 4 *C* and *D*). However, both fractions enriched in *o*-αSyn (#38 and #56) induced a ∼40% lowering in synapsin abundance 6 h postdelivery, reminiscent of the ∼40% reduction seen in the forebrains of 3-mo-old J20×TgI2.2 animals. In contrast, matching SEC fractions derived from *SNCA*-null mice did not lead to significant changes in synapsin protein amounts (Fig. 4 *C* and *D*).

To test whether the exogenous αSyn assemblies transferred into cells required endogenous αSyn to lower synapsin protein amounts, we repeated these experiments using *SNCA*-null primary neurons. In this context, large αSyn species were not able to able to alter the normal synapsin protein profile, whereas the ∼28-kDa αSyn assembly still lowered synapsins (Fig. 4 *C* and *D*). These findings therefore suggest the presence of different functional conformers of αSyn with species requiring template assembly and another that did not. These results also directly demonstrated that *o*-αSyn selectively reduce synapsin proteins in neurons through an unknown mechanism.

αSyn Oligomers Inhibit cAMP Response Element Binding- and Nurr1-Controled Transcription of SYN Genes. Finally, to assess whether *o*-αSyn alter *SYN1* and *SYN2* genes encoding for synapsin-I and -II, we measured the expression of transcripts for *SYN1*, *SYN2*, *CPLX1*, and *CPLX2* (complexins), *SYP*, and *SYT1* (synaptotagmin-I) by real-time quantitative PCR (rt-qPCR) in the forebrain of WT and TgI2.2 mice. Three ages were tested (i.e., 4, 7, and 11 mo of age), because we observed an age-dependent increase of *o*-αSyn during this period (Fig. S6). These analyses did not reveal transgene-driven differences in mRNA expression for any of the genes

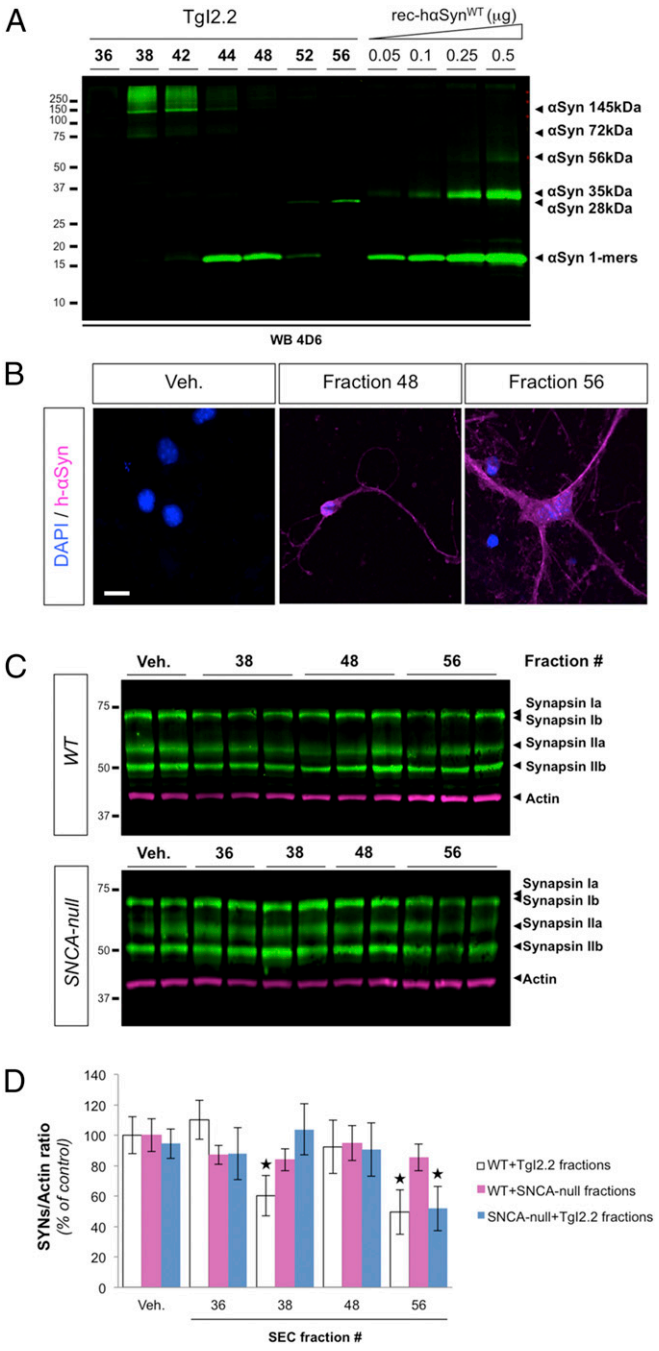

Fig. 4. Intraneuronal delivery of oligomeric αSyn lowers synapsin expression in primary cortical neurons. (*A*) Representative Western blot image illustrating the detection of αSyn species following SEC separation of IC forebrain lysates of 9-mo-old TgI2.2 animals. Increasing amounts of recombinant human αSyn^{WT} was used as internal standard. (*B*) Immunofluorescent labeling of exogenous human αSyn (magenta) delivered intracellularly into cultured primary neurons 6 h postproteotransfection. Nuclei were labeled with DAPI (blue). (Scale bar: 10 μm.) (*C*) Representative Western blot analyses of synapsin isoforms in primary WT (*Upper*) and *SNCA*-null (*Lower*) cortical neurons exposed to SEC fractions containing oligomeric (#38 and #56) or monomeric (#48) αSyn derived from TgI2.2 mice for 6 h. Actin was used as internal standard. (*D*) Densitometry analyses revealed apparent reduction in synapsins in cells treated with oligomeric αSyn but not with monomeric αSyn. (Histogram values represent mean ± SD, ANOVA followed by Student *t* test with Bonferroni correction, $F_{4,\ 50} = 24.930$, $F_{4,\ 50} = 0.819$, and $F_{4,\ 50} = 26.742$ for WT cells + TgI2.2 fractions, WT cells + *SNCA*-null fractions and *SNCA*-null cells + TgI2.2 fractions respectively; $^{\star}P < 0.05$ vs. WT, $n = 6$ animals per group per genotype.) Veh., vehicle.

tested in the youngest group of animals. However, *SYN1* and *SYN2* mRNAs were selectively reduced by ~20–30% at 7 and 11 mo of age in TgI2.2 mice compared with non-Tg littermates (Fig. 5*A*). To demonstrate that *o*-αSyn were directly responsible for this change, we introduced αSyn monomers (#48) or αSyn oligomers (#38 and #56) into cultured cortical neurons using Chariot-mediated delivery and measured the expression of *SYN1*, *SYN2*, *CPLX1*, *CPLX2*, and *SYP* mRNAs 6 h postdelivery. Reminiscent of the in vivo findings, *SYN1* and *SYN2* transcripts were down-regulated by 30–50%, whereas *CPLX1*, *CPLX2*, and *SYP* mRNAs were unchanged (Fig. 5*B*). Using the MRC DBD: Transcription factor prediction database (www.transcriptionfactor.org), we identified putative responsive elements for cAMP response element binding (CREB) and Nurr1 in the 5′UTR/promoter region of *SYN1* and *SYN2* (Fig. 5*C*), two transcription factors known to be suppressed by αSyn (29, 30). Importantly, these sequences are conserved between mouse and human genomes. We then measured the abundance of Nurr1 and the activated form of CREB phosphorylated at serine 133 (pS133-CREB) in forebrain tissues of TgI2.2 mice and found age- and transgene-dependent reductions in both transcription factors between 4 and 11 mo of age (Fig. 5 *D*–*F*). We also confirmed that IC delivery of *o*-αSyn in neurons led to a decrease in pS133-CREB and Nurr1 proteins (Fig. S10*D*). Finally, we performed gene promoter reporter assays in HEK293 cells to demonstrate that CREB and Nurr1 control the transcriptional expression of *SYN1* and *SYN2* genes, respectively. Using the dual luciferase system, we found that forskolin-induced CREB activation up-regulated both mouse and human SYN1 proximal promoter activities (Fig. 5*G*) and that expressing Nurr1 in cells elevated the activity of the human *SYN2* proximal promoter (Fig. 5*H*). Taken together, these results suggest that *o*-αSyn selectively down-regulate *SYN1* and *SYN2* gene expression by inhibiting CREB and Nurr1.

Discussion

A common effort in the field of neurodegenerative diseases is to determine the pathogenic contribution of misfolded proteins once aggregation occurs. With this focus, there has been a paradigm shift toward studying the contribution of soluble, non-fibrillar forms of amyloid proteins, as these assemblies have been proposed to be more toxic than fibrillar species. In AD, intense focus has been set on early aggregates of Aβ and tau, as the fibrillary forms of these proteins have constituted the pathological hallmarks of the disease. Several years ago, however, we reported that disturbances in the abundance of another aggregation-prone amyloid protein, αSyn, might also be involved in AD pathophysiology (18). Because monomeric forms of amyloid proteins are prone to aggregation and because some soluble oligomeric assemblies of αSyn have been reported to be neurotoxic (31–35), we hypothesized that the observed increase in apparent soluble αSyn monomers (18) was accompanied by an elevation of toxic αSyn oligomers, causing the observed decrease in synapsins and the exacerbation of memory deficits triggered by human Aβ and tau.

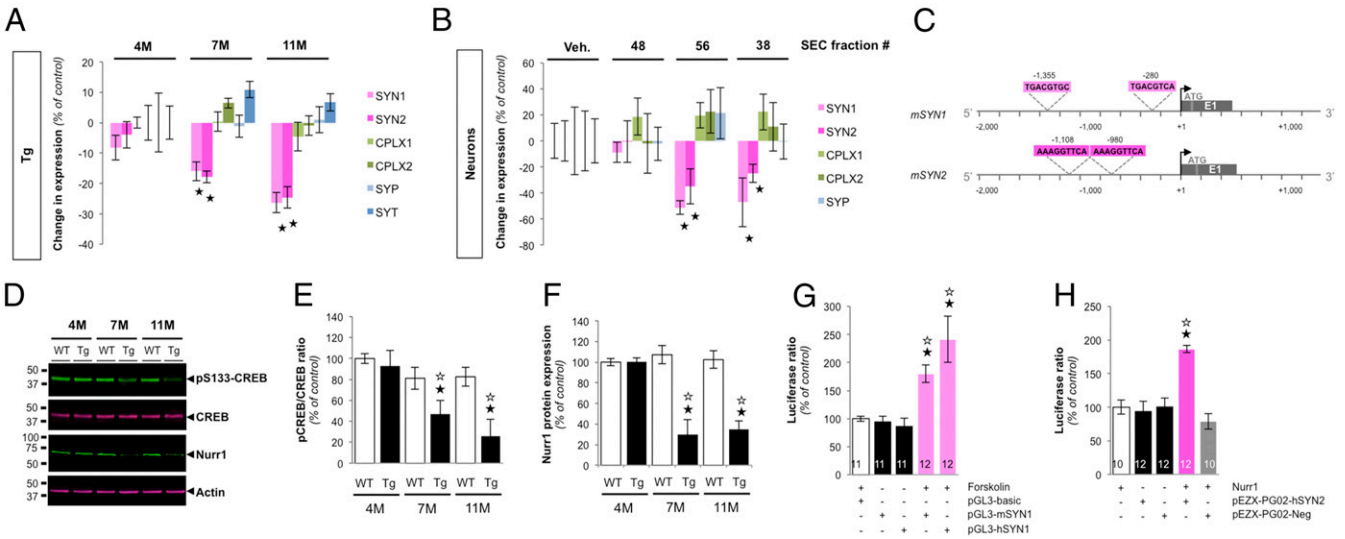

Fig. 5. αSyn oligomers down-regulate *SYN1* and *SYN2* gene expression through CREB and Nurr1. (*A*) Age-dependent changes of *SYN1*, *SYN2*, *CPLX1*, *CPLX2*, *SYP*, and *SYT1* gene expression by rt-qPCR analysis in the forebrain of TgI2.2 mice. Two-way ANOVA revealed a significant effect of transgene ($F = 37.18$, $P < 0.0001$), of age ($F = 21.09$, $P < 0.0001$), and transgene × age interaction ($F = 4.92$, $P = 0.033$) for *SYN1* mRNA. The same analysis revealed a significant effect of transgene ($F = 36.61$, $P < 0.0001$), of age ($F = 18.37$, $P < 0.0001$), and transgene × age interaction ($F = 4.37$, $P = 0.041$) for *SYN2* mRNA. (Histogram values represent mean ± SD, ANOVA followed by Student *t* test with Bonferroni correction, $F_{3,\ 35} = 20.026$ and $F_{3,\ 35} = 18.99$ for *SYN1* and *SYN2*, respectively; $^{\star}P < 0.05$ vs. WT, n = 6–10 animals per age.) (*B*) Changes of *SYN1*, *SYN2*, *CPLX1*, *CPLX2*, *SYP*, and *SYT1* gene expression by rt-qPCR analysis in primary cortical neurons following Chariot-mediated delivery of with isolated αSyn species. (Histogram values represent mean ± SD, ANOVA followed by Student *t* test with Bonferroni correction, $F_{3,\ 24} = 9.173$, $P = 0.0004$ and $F_{3,\ 24} = 6.407$, $P = 0.0013$ for *SYN1* and *SYN2*, respectively; $^{\star}P < 0.05$ vs. WT, $n = 6$ dishes per treatment.) (*C*) Predicted response elements for CREB (light pink) and Nurr1 (dark pink) within mouse *SYN1* and *SYN2* genes. (*D*) Representative Western blot images illustrating the abundance of pS133-CREB, total CREB, Nurr1, and actin in forebrain lysates of 4-, 7-, and 11-mo-old WT and TgI2.2 mice. (*E* and *F*) Densitometry analyses revealed age-dependent reductions in the phosphorylated (p)CREB/CREB ratio (*E*) and in Nurr1 (*F*) protein amounts. Two-way ANOVA revealed a significant effect of transgene ($F = 168.67$, $P < 0.0001$), of age ($F = 129.39$, $P < 0.0001$), and transgene × age interaction ($F = 72.74$, $P < 0.0001$) for the pCREB/CREB ratio. The same analysis revealed a significant effect of transgene ($F = 91.34$, $P < 0.0001$), of age ($F = 22.09$, $P < 0.0001$), and transgene × age interaction ($F = 29.93$, $P < 0.0001$) for Nurr1. (Histogram values represent mean ± SD, two-way ANOVA followed by Student *t* test with Bonferroni correction, $F_{3,\ 30} = 130.886$ and $F_{3,\ 30} = 49.870$ for pCREB/CREB and Nurr1, respectively; $^{\star}P < 0.05$ vs. WT, $^{\star}P < 0.05$ vs. 4-mo-old TgI2.2 mice, n = 5–6 animals per group per genotype.) (*G* and *H*) Dual luciferase gene promoter reporter assay revealed that the activity of mouse and human SYN1 (*G*) and SYN2 (*H*) promoters is positively modulated by CREB and Nurr1, respectively. Treating cells with 10 μM forskolin activated CREB as assessed by phosphorylation at S133 and nuclear translocation. (Histogram values represent mean ± SD, ANOVA followed by Student *t* test with Bonferroni correction, $F_{5,\ 57} = 120.67$ and $F_{5,\ 56} = 112.48$ for SYN1 and SYN2 promoters, respectively; $^{\star}P < 0.05$ vs. empty vector, $^{\star}P < 0.05$ vs. stimulated cells, n = 10–12 dishes per group.) M, months; Veh., vehicle.

Distinct Soluble αSyn Species Linked to AD-Associated Impairment. In this follow-up study, we identified putative multimers of two monomeric αSyn species of 14 and 17 kDa that included putative dimers (~28 and 35 kDa), and tetramers (~56 kDa) using a combination of biochemical techniques. The recognition of this pattern suggests the possible existence of two likely pathways for the aggregation of αSyn in vivo, a principle first suggested by molecular modeling of αSyn aggregates (36) and recently integrated into the proposed mechanisms of αSyn aggregation and propagation (3). This hypothesis is further supported by the existence of divergent detections of *o*-αSyn by the homotypic LB509 and heterotypic LB509-A11 pairs used for the ELISA studies, as recently reported for Aβ (37). If correct, the human samples showing detection with both homotypic and heterotypic pairs would contain both conformers. The disease significance to this observation is unclear at this time because of the small numbers of brain specimens composing all three categories ($LB509^+$, $A11^+$, and $LB509/A11^+$) and because of the creation of necessary cut-offs, but certainly warrants larger studies to examine the functional role of these entities of αSyn. Although other groups have provided evidence that ~35-kDa SDS-resistant αSyn dimers can be detected in brain tissue (24, 38, 39), we speculate that the unique experimental biological specimens used (i.e., human brain tissue with elevated expression of αSyn combined with an absence of LB pathology) allowed us to detect apparent multimers of 14- and 17-kDa αSyn monomers.

We also believe that the detection of these various soluble forms was only possible using the antibody 4D6, which we recognized to display enhanced sensitivity toward *o*-αSyn following relaxation or denaturation of αSyn molecules, even compared with antibodies specifically raised to detect *o*-αSyn, such as Syn33 and F8H7. With these conditions, biochemical evidence suggested that *o*-αSyn accumulated intracellularly in AD brains compared with age-matched controls, whereas EC *o*-αSyn species were less abundant in the AD group. A possible interpretation of these results consists in *o*-αSyn being expelled from the cytosol of neurons under normal conditions, perhaps as a self-regulated protective mechanism, thereby creating an equilibrium between IC and EC compartments. In AD, this balance would be disrupted, facilitating the intraneuronal accumulation of αSyn oligomers. Given the emerging focus on prion-like spreading of amyloid aggregates, it remains to be determined whether the species studied here can propagate from cell-to-cell via the EC space as it was reported for dissociated fibrillar assemblies (40, 41).

In addition to the accumulation of an ~56-kDa αSyn species in IC fractions of AD brain tissues, the levels of this possible tetramer of the 14-kDa monomeric αSyn were inversely correlated to episodic and semantic memory performance. Although the exact structure and folding of endogenous αSyn remains highly controversial (12, 14, 15), we posit that the ~56-kDa αSyn assembly detected in our studies is unlikely to correspond to the ~55- to 60-kDa tetrameric αSyn first identified by the Selkoe group (13, 15, 17) because their biophysical properties appear different (notably their relative stability in presence of SDS) (42). If it were the case nonetheless, our findings suggest that an abnormal accumulation of these so-called "physiological multimers" might be deleterious for neuronal function and cognition.

Finally, on this topic, it is worth stressing that monomeric αSyn also correlated with cognitive function, and could therefore be a determining factor in modulating cognition as well.

Synapsin-I/II Lowering and Cognitive Deficits in AD and Animal Models. Moreover, we documented that the amounts of *o*-αSyn detected under native conditions positively correlated with reductions in synapsin abundance in AD brain specimens. This relationship appeared to be relatively specific to the *o*-αSyn/synapsins pair, as similar analyses with SYN did not reveal an association with soluble *o*-αSyn levels.

We also found that total synapsin-I/II levels were correlated to the level of episodic memory within the Religious Orders Study AD cohort examined. Our results are consistent with existing reports showing that reduction in synapsin-I gene expression induced by increased DNA methylation is linked to cognitive aging in rodents (43) and that ablation of either the synapsin-I or synapsin-II gene causes age-dependent cognitive impairment in mice involving emotional and spatial memory (44). Of note, 12- to 14-mo-old *SYN1*-null mice display neuronal loss and gliosis in the hippocampus and neocortex (44) further highlighting the importance of putative changes in synapsin expression in AD. In addition, *SYN1* and *SYN2* loss-of function mutations in humans were recently shown to be causative for autism spectrum disorder (45, 46), associated with excitatory/inhibitory imbalance and epileptic seizures (47). Strikingly, both of these changes have also emerged as prominent features of mouse modeling AD (48, 49) and early AD (50). Considering the results presented in this study, our previous results showing a ~60% reduction in synapsins associated with the increase in soluble αSyn species in AD (18) and the growing recognition of network disturbance associated with AD (49–51), we postulate that the lowering of synapsins-I and -II observed in AD might mediate the enhancement of memory deficits triggered by *o*-αSyn.

To determine whether an elevation in soluble h-αSyn^{WT} oligomers could induce a selective reduction in synapsins in a mouse model of AD, we generated a bigenic mouse line expressing human Aβ and h-αSyn^{WT}, based on earlier observations indicating that Aβ and αSyn can potentiate the aggregation of each other in vivo (22). At 3 mo of age when pathological lesions are absent, forebrain *o*-αSyn were increased by ~fourfold in J20×TgI2.2 bigenic mice compared with TgI2.2 littermates, but monomeric αSyn was unchanged. This marked rise of *o*-αSyn was associated with selective reductions in synapsin-I/II proteins and with profound deficits in learning and memory retention. This observation contrasts with earlier results showing that memory retention in 6-mo-old bigenic hAPP/hSYN (J9×D line) and in hAPP mice were identical (22). We speculate that this apparent discrepancy between these two studies might be because of the fact that hSYN-line D mice elicit LB inclusions as early as 3 mo of age and that motor function is compromised in bigenic hAPP/hSYN at 6 mo (52). Conversely, TgI2.2 mice do not develop pathological lesions (27) and do not display apparent motor deficits during behavioral testing as assessed by animal speed and distance run during the task.

In this context, it is worth stressing a couple of important points related to the animal models used. First, recent studies reported that the overexpression of the A30P mutant of human αSyn in APP/PS1 Tg mice, another model of AD, led to a lowering of Aβ deposition and to synaptic abnormalities suggestive of synapse loss (53). The alterations in synaptic proteins observed in 3-mo-old bigenic J20×TgI2.2 mice appear reminiscent of those reported by Bachhuber et al. despite qualitative differences. However, our results indicate that overexpression of h-αSyn^{WT} worsens cognitive deficits in absence of deposited Aβ and αSyn, although it remains unknown whether the changes reported for APP/PS1 × αSyn^{A30P} bigenic animals translate into cognitive deficits. Furthermore, it also remains unclear whether h-αSyn^{WT} can alter Aβ-induced phenotypes, considering the distinct properties of αSyn^{A30P} (54). Second, despite previous evidence reporting the association of Aβ oligomers and cognitive deficits in J20 mice before plaque formation (55), the in vivo results presented here cannot rule out the possibility that the potentiation of the memory impairments seen in J20×TgI2.2 bigenic mice is a result of the overexpression of APP in these mice (i.e., ~threefold over endogenous APP). However, recent analyses using single-cell qPCR revealed that individual neurons in sporadic AD can harbor an averaged copy number for *APP* of 3.8–4 (up to 12 copies) over control samples (56), suggesting that the threefold elevation of APP seen in J20 mice might actually be relevant to AD. That said, future studies using newly described APP knockin animals will be needed to address whether the overexpression of αSyn can also alter the phenotype of these lines (57).

Overall, our genetic experiment replicated the changes observed in AD brain tissue and supports the notion that an increase in *o*-αSyn is associated with synapsin-I/II lowering and the potentiation of Aβ-induced cognitive impairment. It is also important to note that the J20×TgI2.2 bigenic model was created to selectively enhance αSyn oligomerization, and as such might not reproduce changes mediated by increased levels of αSyn transcripts and of the monomeric protein. Future studies with new animal models will be necessary to fully address their role in AD.

Dependence on Endogenous αSyn for Exogenous *o*-αSyn to Induce Reductions in Synapsin Abundance. To directly demonstrate that *o*-αSyn induced a selective reduction in synapsin protein abundance, we used an in vitro approach to deliver exogenous αSyn species isolated from brain tissue of cognitively impaired TgI2.2 mice into primary neurons. Although intraneuronal delivery of exogenous αSyn monomers did not alter synapsin-I/II protein amounts compared with vehicle or to equivalent SEC fractions using *SNCA*-null lysates, IC delivery of *o*-αSyn fractions in cultured neurons caused a 40–50% reduction in synapsins-I and -II within 6 h. Because of accumulating evidence reporting prion-like propagation of small fibrillar amyloid aggregates (58–61), we asked whether endogenous αSyn was required for the tested exogenous *o*-αSyn to perturb synapsins-I and -II protein abundance. Our results indicated that larger *o*-αSyn species lost their ability to reduce synapsins when introduced into *SNCA*-null neurons lacking αSyn, whereas smaller *o*-αSyn assemblies did not depend on endogenous αSyn to lower synapsins, reminiscent of prion-like mechanisms. In agreement with earlier reports (35, 40, 62), these findings therefore suggested the presence of different functional conformers of αSyn with species requiring template assembly and others that did not. On the one hand, the fact that both αSyn aggregates trigger the same cellular change is surprising, as one would perhaps predict differential alterations in neuronal biology induced by each species. On the other hand, this apparent conversion on synapsin regulation could be viewed as a central and essential mechanism induced by soluble αSyn aggregates. As new tools and additional assemblies are isolated, future studies should be able to directly address this hypothesis.

***o*-αSyn Down-Regulate *SYN1* and *SYN2* Gene Expression Through CREB and Nurr1.** Finally, at a molecular level, we revealed that the reduction in synapsin proteins occurs in parallel to a selective down-regulation of the transcription of *SYN1* and *SYN2* genes in vivo when oligomeric αSyn species are present and in vitro when isolated αSyn oligomers are introduced intraneuronally. These results are consistent with the publicly available RNA sequencing data (NCBI Gene Expression Omnibus accession no. GSE70368) from recent studies using mouse primary midbrain neurons infected with αSyn (30). Upon αSyn overexpression, transcripts for *SYN1*, *SYN2*, and *SYN3* were down-regulated by ∼30–70%, whereas *CPLX1*, *CPLX2*, *SYP*, and *SYT1* mRNAs were unchanged compared with control neurons. Although the presence of *o*-αSyn was not disclaimed in these studies, we advance that these changes might be a result of the presence of αSyn oligomers based on our own in vitro results. Using predictive databases, we found that human and mouse *SYN1* and *SYN2* promoters contained conserved putative responsive elements for CREB and Nurr1, respectively, two transcription factors involved in αSyn-mediated toxicity (29, 30, 63). We then found that the protein abundance of pS133-CREB and Nurr1 was decreased in association with the age-dependent accumulation of αSyn oligomers in TgI2.2 mice and following intraneuronal delivery of *o*-αSyn. Finally, we confirmed that CREB and Nurr1 are active enhancers of *SYN1* and *SYN2* promoter activities. Other transcription factors have been recently identified to positively regulate *SYN1* promoter activity, including Sp1 at sites immediately distal and proximal from the proximal CREB site (64), which raises the possibility that Sp1 and CREB might cooperate to control *SYN1* expression.

To conclude, we believe that soluble αSyn species are an intrinsic component of the sequence of events leading to dementia in AD, thereby exacerbating the severity of cognitive impairment, perhaps mediated by a selective lowering of synapsins. We also trust that these findings also apply to other synucleinopathies, in particular dementia with LBs. Although further studies are required to elucidate the mechanism governing the up-regulation of αSyn, this αSyn/synapsin axis might constitute an intriguing therapeutic target with the overarching goal to attenuate cognitive decline in patients at early stages of the disease.

Methods

Human Brain Tissue. Brain specimens and subject characteristics were described previously (65). The Religious Orders Study was approved by the Institutional Review Board of Rush University Medical Center and all participants gave informed consent, signed an Anatomical Gift Act for organ donation, and signed a repository consent to allow data and biospecimen sharing. The University of Minnesota Institutional Review Board approved this study.

Transgenic Animals. Three Tg lines were used: (*i*) TgI2.2 mice expressing the WT form of human αSyn under the control of the mouse prion promoter (27), (*ii*) *SNCA*-null mice (66), and (*iii*) J20 mice (21). Bigenic J20×TgI2.2 mice resulted from the mating of TgI2.2 and J20 mice. All lines used were in the C57BL6 background strain. Both male and female animals were used in biochemical studies and BCM behavioral testing. All animal procedures and studies were reviewed and approved by the University of Minnesota Institutional Animal Care and Use Committee and Institutional Review Board.

Primary Cell Cultures. Mouse cortical cultures of neurons were prepared and used as described previously (67).

Protein Extractions. Protocols for protein extractions are described previously (67).

IC Delivery of Human αSyn Oligomers. Selected SEC fractions enriched or devoid in identified soluble αSyn species were coincubated for 30 min at 4 °C with 6 μL/μg of Chariot (Actif Motif). Mixtures were applied to the conditioned media of cells for 90 min at 37 °C.

SEC. Protein separation was achieved as previously described (67).

Western Blotting and Quantification. Experimental settings were described previously (18, 67).

Spatial Reference Memory Assessments. Experiments were performed as described previously (18, 67).

ACKNOWLEDGMENTS. We thank Kenji Kanamura, Hoa Nguyen, and Chani Maher (Becker) for technical help, and the participants in the Religious Orders Study. This work was supported in part by NIH Grant R01AG044342, research Grant 4185-9227-14, and start-up funds from the University of Minnesota Foundation (to S.E.L.); and NIH Grants P30AG10161 and R01AG15819 (to D.A.B.).

1. Lasagna-Reeves CA, et al. (2011) Tau oligomers impair memory and induce synaptic and mitochondrial dysfunction in wild-type mice. *Mol Neurodegener* 6:39.
2. Larson ME, Lesné SE (2012) Soluble Aβ oligomer production and toxicity. *J Neurochem* 120:125–139.
3. Lashuel HA, Overk CR, Oueslati A, Masliah E (2013) The many faces of α-synuclein: From structure and toxicity to therapeutic target. *Nat Rev Neurosci* 14:38–48.
4. Bendor JT, Logan TP, Edwards RH (2013) The function of α-synuclein. *Neuron* 79: 1044–1066.
5. Diao J, et al. (2013) Native α-synuclein induces clustering of synaptic-vesicle mimics via binding to phospholipids and synaptobrevin-2/VAMP2. *eLife* 2:e00592.
6. Rizo J, Südhof TC (2012) The membrane fusion enigma: SNAREs, Sec1/Munc18 proteins, and their accomplices—Guilty as charged? *Annu Rev Cell Dev Biol* 28:279–308.
7. Burré J, et al. (2010) Alpha-synuclein promotes SNARE-complex assembly in vivo and in vitro. *Science* 329:1663–1667.
8. Nemani VM, et al. (2010) Increased expression of alpha-synuclein reduces neurotransmitter release by inhibiting synaptic vesicle reclustering after endocytosis. *Neuron* 65:66–79.

9. Choi BK, et al. (2013) Large α-synuclein oligomers inhibit neuronal SNARE-mediated vesicle docking. *Proc Natl Acad Sci USA* 110:4087–4092.
10. Cesca F, Baldelli P, Valtorta F, Benfenati F (2010) The synapsins: Key actors of synapse function and plasticity. *Prog Neurobiol* 91:313–348.
11. Roy S, Winton MJ, Black MM, Trojanowski JQ, Lee VM (2007) Rapid and intermittent cotransport of slow component-b proteins. *J Neurosci* 27:3131–3138.
12. Burré J, et al. (2013) Properties of native brain alpha-synuclein. *Nature* 498:E4–E6; discussion E6–7.
13. Selkoe D, et al. (2014) Defining the native state of α-synuclein. *Neurodegener Dis* 13: 114–117.
14. Fauvet B, et al. (2012) α-Synuclein in central nervous system and from erythrocytes, mammalian cells, and *Escherichia coli* exists predominantly as disordered monomer. *J Biol Chem* 287:15345–15364.
15. Bartels T, Choi JG, Selkoe DJ (2011) α-Synuclein occurs physiologically as a helically folded tetramer that resists aggregation. *Nature* 477:107–110.
16. Davidson WS, Jonas A, Clayton DF, George JM (1998) Stabilization of alpha-synuclein secondary structure upon binding to synthetic membranes. *J Biol Chem* 273: 9443–9449.
17. Dettmer U, Newman AJ, Luth ES, Bartels T, Selkoe D (2013) In vivo cross-linking reveals principally oligomeric forms of α-synuclein and β-synuclein in neurons and non-neural cells. *J Biol Chem* 288:6371–6385.
18. Larson ME, et al. (2012) Soluble α-synuclein is a novel modulator of Alzheimer's disease pathophysiology. *J Neurosci* 32:10253–10266.
19. Lim Y, Kehm VM, Li C, Trojanowski JQ, Lee VM (2010) Forebrain overexpression of alpha-synuclein leads to early postnatal hippocampal neuron loss and synaptic disruption. *Exp Neurol* 221:86–97.
20. Scott DA, et al. (2010) A pathologic cascade leading to synaptic dysfunction in alpha-synuclein-induced neurodegeneration. *J Neurosci* 30:8083–8095.
21. Mucke L, et al. (2000) High-level neuronal expression of abeta 1-42 in wild-type human amyloid protein precursor transgenic mice: Synaptotoxicity without plaque formation. *J Neurosci* 20:4050–4058.
22. Masliah E, et al. (2001) beta-amyloid peptides enhance alpha-synuclein accumulation and neuronal deficits in a transgenic mouse model linking Alzheimer's disease and Parkinson's disease. *Proc Natl Acad Sci USA* 98:12245–12250.
23. Sengupta U, et al. (2015) Pathological interface between oligomeric alpha-synuclein and tau in synucleinopathies. *Biol Psychiatry* 78:672–683.
24. Tsigelny IF, et al. (2008) Mechanisms of hybrid oligomer formation in the pathogenesis of combined Alzheimer's and Parkinson's diseases. *PLoS One* 3:e3135.
25. Kayed R, et al. (2007) Fibril specific, conformation dependent antibodies recognize a generic epitope common to amyloid fibrils and fibrillar oligomers that is absent in prefibrillar oligomers. *Mol Neurodegener* 2:18.
26. Kayed R, et al. (2003) Common structure of soluble amyloid oligomers implies common mechanism of pathogenesis. *Science* 300:486–489.
27. Lee MK, et al. (2002) Human alpha-synuclein-harboring familial Parkinson's disease-linked Ala-53 –> Thr mutation causes neurodegenerative disease with alpha-synuclein aggregation in transgenic mice. *Proc Natl Acad Sci USA* 99:8968–8973.
28. Clinton LK, Blurton-Jones M, Myczek K, Trojanowski JQ, LaFerla FM (2010) Synergistic interactions between Abeta, tau, and alpha-synuclein: Acceleration of neuropathology and cognitive decline. *J Neurosci* 30:7281–7289.
29. Decressac M, et al. (2012) α-Synuclein-induced down-regulation of Nurr1 disrupts GDNF signaling in nigral dopamine neurons. *Sci Transl Med* 4:163ra156.
30. Volakakis N, et al. (2015) Nurr1 and retinoid X receptor ligands stimulate Ret signaling in dopamine neurons and can alleviate α-synuclein disrupted gene expression. *J Neurosci* 35:14370–14385.
31. Winner B, et al. (2011) In vivo demonstration that alpha-synuclein oligomers are toxic. *Proc Natl Acad Sci USA* 108:4194–4199.
32. Danzer KM, et al. (2007) Different species of alpha-synuclein oligomers induce calcium influx and seeding. *J Neurosci* 27:9220–9232.
33. Colla E, et al. (2012) Accumulation of toxic α-synuclein oligomer within endoplasmic reticulum occurs in α-synucleinopathy in vivo. *J Neurosci* 32:3301–3305.
34. Outeiro TF, et al. (2008) Formation of toxic oligomeric alpha-synuclein species in living cells. *PLoS One* 3:e1867.
35. Peelaerts W, et al. (2015) α-Synuclein strains cause distinct synucleinopathies after local and systemic administration. *Nature* 522:340–344.
36. Tsigelny IF, et al. (2007) Dynamics of alpha-synuclein aggregation and inhibition of pore-like oligomer development by beta-synuclein. *FEBS J* 274:1862–1877.
37. Liu P, et al. (2015) Quaternary structure defines a large class of amyloid-β oligomers neutralized by sequestration. *Cell Reports* 11:1760–1771.
38. Rockenstein E, et al. (2014) Accumulation of oligomer-prone α-synuclein exacerbates synaptic and neuronal degeneration in vivo. *Brain* 137:1496–1513.
39. Kahle PJ, et al. (2001) Selective insolubility of alpha-synuclein in human Lewy body diseases is recapitulated in a transgenic mouse model. *Am J Pathol* 159:2215–2225.
40. Luk KC, et al. (2012) Intracerebral inoculation of pathological α-synuclein initiates a rapidly progressive neurodegenerative α-synucleinopathy in mice. *J Exp Med* 209: 975–986.
41. Volpicelli-Daley LA, Luk KC, Lee VM (2014) Addition of exogenous α-synuclein preformed fibrils to primary neuronal cultures to seed recruitment of endogenous α-synuclein to Lewy body and Lewy neurite-like aggregates. *Nat Protoc* 9:2135–2146.
42. Dettmer U, et al. (2015) Parkinson-causing α-synuclein missense mutations shift native tetramers to monomers as a mechanism for disease initiation. *Nat Commun* 6:7314.
43. Haberman RP, Quigley CK, Gallagher M (2012) Characterization of CpG island DNA methylation of impairment-related genes in a rat model of cognitive aging. *Epigenetics* 7:1008–1019.
44. Corradi A, et al. (2008) Synapsin-I- and synapsin-II-null mice display an increased age-dependent cognitive impairment. *J Cell Sci* 121:3042–3051.
45. Fassio A, et al. (2011) SYN1 loss-of-function mutations in autism and partial epilepsy cause impaired synaptic function. *Hum Mol Genet* 20:2297–2307.
46. Corradi A, et al. (2014) SYN2 is an autism predisposing gene: Loss-of-function mutations alter synaptic vesicle cycling and axon outgrowth. *Hum Mol Genet* 23:90–103.
47. Giovedí S, Corradi A, Fassio A, Benfenati F (2014) Involvement of synaptic genes in the pathogenesis of autism spectrum disorders: The case of synapsins. *Front Pediatr* 2:94.
48. Palop JJ, Mucke L (2010) Synaptic depression and aberrant excitatory network activity in Alzheimer's disease: Two faces of the same coin? *Neuromolecular Med* 12:48–55.
49. Verret L, et al. (2012) Inhibitory interneuron deficit links altered network activity and cognitive dysfunction in Alzheimer model. *Cell* 149:708–721.
50. Vossel KA, et al. (2013) Seizures and epileptiform activity in the early stages of Alzheimer disease. *JAMA Neurol* 70:1158–1166.
51. Mucke L, Selkoe DJ (2012) Neurotoxicity of amyloid β-protein: Synaptic and network dysfunction. *Cold Spring Harb Perspect Med* 2:a006338.
52. Masliah E, et al. (2000) Dopaminergic loss and inclusion body formation in alpha-synuclein mice: Implications for neurodegenerative disorders. *Science* 287:1265–1269.
53. Bachhuber T, et al. (2015) Inhibition of amyloid-β plaque formation by α-synuclein. *Nat Med* 21:802–807.
54. Burré J, Sharma M, Südhof TC (2015) Definition of a molecular pathway mediating α-synuclein neurotoxicity. *J Neurosci* 35:5221–5232.
55. Cheng IH, et al. (2007) Accelerating amyloid-beta fibrillization reduces oligomer levels and functional deficits in Alzheimer disease mouse models. *J Biol Chem* 282: 23818–23828.
56. Bushman DM, et al. (2015) Genomic mosaicism with increased amyloid precursor protein (APP) gene copy number in single neurons from sporadic Alzheimer's disease brains. *eLife* 4:4.
57. Saito T, et al. (2014) Single App knock-in mouse models of Alzheimer's disease. *Nat Neurosci* 17:661–663.
58. Walker LC, Jucker M (2015) Neurodegenerative diseases: Expanding the prion concept. *Annu Rev Neurosci* 38:87–103.
59. Jucker M, Walker LC (2013) Self-propagation of pathogenic protein aggregates in neurodegenerative diseases. *Nature* 501:45–51.
60. Eisenberg D, Jucker M (2012) The amyloid state of proteins in human diseases. *Cell* 148:1188–1203.
61. Guo JL, Lee VM (2014) Cell-to-cell transmission of pathogenic proteins in neurodegenerative diseases. *Nat Med* 20:130–138.
62. Luk KC, et al. (2016) Molecular and biological compatibility with host alpha-synuclein influences fibril pathogenicity. *Cell Reports* 16:3373–3387.
63. Decressac M, Volakakis N, Björklund A, Perlmann T (2013) NURR1 in Parkinson disease—From pathogenesis to therapeutic potential. *Nat Rev Neurol* 9:629–636.
64. Paonessa F, Latifi S, Scarongella H, Cesca F, Benfenati F (2013) Specificity protein 1 (Sp1)-dependent activation of the synapsin I gene (SYN1) is modulated by RE1-silencing transcription factor (REST) and 5′-cytosine-phosphoguanine (CpG) methylation. *J Biol Chem* 288:3227–3239.
65. Lesné SE, et al. (2013) Brain amyloid-β oligomers in ageing and Alzheimer's disease. *Brain* 136:1383–1398.
66. Abeliovich A, et al. (2000) Mice lacking alpha-synuclein display functional deficits in the nigrostriatal dopamine system. *Neuron* 25:239–252.
67. Larson M, et al. (2012) The complex PrP(c)-Fyn couples human oligomeric Aβ with pathological tau changes in Alzheimer's disease. *J Neurosci* 32:16857-71a.
68. Bennett DA, Schneider JA, Arvanitakis Z, Wilson RS (2012) Overview and findings from the religious orders study. *Curr Alzheimer Res* 9:628–645.
69. Small GW, et al. (2000) Cerebral metabolic and cognitive decline in persons at genetic risk for Alzheimer's disease. *Proc Natl Acad Sci USA* 97:6037–6042.
70. Desikan RS, et al.; Alzheimer's Disease Neuroimaging Initiative (2010) Selective disruption of the cerebral neocortex in Alzheimer's disease. *PLoS One* 5:e12853.
71. Wilson RS, et al. (2002) Individual differences in rates of change in cognitive abilities of older persons. *Psychol Aging* 17:179–193.
72. Bennett DA, et al. (2006) Decision rules guiding the clinical diagnosis of Alzheimer's disease in two community-based cohort studies compared to standard practice in a clinic-based cohort study. *Neuroepidemiology* 27:169–176.
73. Bennett DA, Schneider JA, Wilson RS, Bienias JL, Arnold SE (2004) Neurofibrillary tangles mediate the association of amyloid load with clinical Alzheimer disease and level of cognitive function. *Arch Neurol* 61:378–384.
74. Bennett DA, Schneider JA, Bienias JL, Evans DA, Wilson RS (2005) Mild cognitive impairment is related to Alzheimer disease pathology and cerebral infarctions. *Neurology* 64:834–841.
75. Lesné S, et al. (2006) A specific amyloid-beta protein assembly in the brain impairs memory. *Nature* 440:352–357.
76. Sherman MA, Lesné SE (2011) Detecting aβ*56 oligomers in brain tissues. *Methods Mol Biol* 670:45–56.
77. Sunyer B, Patil S, Höger H, Lubec G (2007) Barnes maze, a useful task to assess spatial reference memory in the mice. *Protoc Exch*, 10.1038/nprot.2007.390.